

AN INNOVATIVE DISTRIBUTED BASE-ISOLATION SYSTEM FOR MASONRY BUILDINGS: THE REINFORCED CUT-WALL

Mauro SASSU¹ And Christian RICCI²

SUMMARY

The article reports the results of experimental tests conducted on an innovative masonry-building seismic isolator, named "reinforced cut-wall". The system is simple to construct and inexpensive to implement, yet delivers high static performance. It is made up of a layer of low load-bearing capacity mortar and an underlying sheet of elastomer waterproofing interposed between the base of the walls and the foundation head and reinforced by a series of vertical steel rods anchored to both the wall and foundation by concrete castings. The experimental trials were conducted on pairs of cellular blocks, 20x20x50 cm, separated by a 5 cm-thick layer of mortar and 3mm elastomer sheathing; the rods used ranged from 8 to 12 mm in diameter. Such specimens were subjected to a constant vertical force, simulating the actions of permanent in-service loads, and a cyclic history of horizontal forces (max. 0.4 times the vertical load), representing an earthquake. Test results, expressed as a series of hysteresis diagrams, reveal a high degree of energy dissipation, attributable to the malt-elastomer joint, and efficient elastic recovery due to the reinforcing bars which also furnish suitable vertical load-bearing capacity. Numerical analyses, conducted by means of a rheological model calibrated with the help of the test results and applied to the case of a simple masonry building, have confirmed the high-level performance of the proposed seismic isolating system.

INTRODUCTION

Background

The idea of placing a vibration filter at the base of masonry buildings to absorb the energy of seismic shocks dates back to at least the turn of the century. Actually, practices adopted on empirical grounds date back much earlier, such as the ancient Chinese who used to place a deformable layer between the ground and house foundations (Buckle 1990) (Zhou 1993), a technique taken up by L. Wright in 1921 in the celebrated Tokyo Imperial Hotel (Arnold 1989). However, specific scientific proposals for isolating masonry structures from the ground have aimed to combine mechanical efficiency with ease of application and economy of components compatible with the "poor" building systems in which they are to be inserted. Some examples (fig. 1) from the early 1900s include the proposal by Calantariet (Olariu 1994), which calls for interposing a layer of talcum and sand between the foundation and masonry base and J. Bechtold's proto-structure (Zhou 1998), made up of a stiff plate sliding over rollers, upon which the building was then laid (analogous to the cylindrical hinges discovered at the foot of some one-storey Chinese buildings damaged by earthquakes). Such design solutions call for seismic isolation systems arranged uniformly around a structure's base, and can therefore be classified as "distributed systems". An alternative strategy is to position a series of support devices in suitable points along the foundation head, whence the designation "localized" isolation systems. While the former normally offer the advantage of a more uniform distribution of the consequent passive-type dynamic control effects throughout the entire building, the second can generally be applied with specially developed support devices or prefabricated

¹ Dept of Structural Engineering, University of Pisa (Italy) fax: ++39.050.554597 e-mail: sassum@ing.unipi.it

² Dept of Structural Engineering, University of Pisa (Italy) fax: ++39.050.554597 e-mail: sassum@ing.unipi.it

components, which can in many cases be more easily retrofitted to existing buildings or their most significant sections.

The "reinforced cut-wall" proposal

The seismic isolation technique dealt with here stems from a recent proposal (Sassu 1999) for a system of the distributed type, called "reinforced cut-wall". It consists of (fig. 2) a layer of mortar of rather modest mechanical properties overlaying waterproof elastomer sheathing laid between the foundation and base of the masonry walls to be isolated. Both layers are moreover reinforced by a series of vertical metal rods anchored to the cast-concrete foundation and building's wall base.

The design of the mortar joint is such that it will remain integral when subjected to low-level seismic actions, but will crack in the face of high-intensity earthquakes, thereby dissipating the mechanical energy of the tremors. The elastomer layer instead has a two-fold function: firstly, to prevent the rise of humidity through capillarity, and secondly, to aid the mortar in dissipating mechanical energy by slipping in the horizontal plane. Lastly, the suitably dimensioned metal rods serve to furnish the necessary elastic restraint for the building to return to its original configuration after cessation of the oscillations, as well as main vertical load-bearing capacity.

The design of the described seismic isolation system moreover enables construction to be carried out through the assembly of prefabricated blocks containing the reinforcing bars, mortar layer and elastomer sheath. Therefore, the operations to be performed on-site are limited to casting the concrete for consolidating the system's lower portion with the foundation, and sealing the sheath along the borders of the prefabricated elements. Such a procedure enables better control of the quality of the energy-dissipating mortar layer, whose strength must be proportioned according to the desired elastic limit-state actions. In order to permit major relative displacements between foundation and masonry panel, it has been also designed an alternative version of the system (*large displacement version*), where the weak mortar is extended into the upper holes connected to wall's base, containing completely the superior part of the steel bars. At present we referee about experimental tests on the first type of base isolator (*small displacement version*).

EXPERIMENTAL TESTS

A first series of experimental trials were carried out on 12 sample block pairs. The specimens (fig. 4) were constructed from two cellular blocks, 20x20x50 cm., each bearing holes for inserting the reinforcing bars and fitted together with an intervening 5 cm-layer of mortar and underlying 3 mm-thick elastomer sheath. Two different types of mortar were tested: lime mortar (type A) and a 1:3 mixture of mortar and concrete (type B). Traditional enhanced-adherence concrete reinforcing rods, whose diameter was varied from 8, 10 and 12 mm, were arranged perpendicular to the mortar-elastomer layer and set in groups of two or four per hole and consolidated with cast concrete. The samples were introduced into the testing apparatus, as per the scheme presented in figure 3. Each was subjected to constant axial load by the action of two prestressed high strength steel rods controlled by two cylindrical dynamometers arranged co-axially to the rods. This load was designed to simulate the presence of the in-service vertical loads experienced by the walls. In addition to this, a shearing load was produced by a 100 KN single-action oil-pressure jack governed by a hydraulic pump able to apply variable load histories over time. This load was intended to simulate the cyclic actions produced by a seismic disturbance. Displacement readings were effected by means of 3 inductive transducers (tol. +/- .001 mm) placed on the vertical faces of the samples to measure the components of relative motion in the plane of the jacks between base and summit. Moreover, each dynamometer was fitted with 4 unidirectional strain gauges.

Conventional crushing tests were first performed to assess the strength of each component (block - cast concrete - mortar - steel bars). Then, samples 1 and 4 were subjected to preliminary measurements under conditions designated as "empty", i.e., in the absence of the mortar isolating layer, and subjected to a maximum vertical load of 3.0 N/mm², obtaining proper stress-strain curves, denoting satisfactory mechanical behavior (fig. 5).

These were carried out to assess both the effect of the prestressing rods on the test itself and the load-bearing capacity of the vertical reinforcement in response to the combined compressive and bending stress, as well as their sensitivity to any elastic instability phenomena or geometric non-linearity due to $P-\delta$ effects. In order to account for any deformation effects due to viscosity, each specimen was then subjected to a first series of experimental trials consisting of 6 cyclic tests, each of which was represented by a brief loading-unloading cycle with a constant-intensity vertical load of 0.5 N/mm².

Subsequently, the mortar joint was repaired and a second test series performed, also consisting of 6 identical loading-unloading cycles with a vertical pressure of 1.0 N/mm². In both cases the maximum horizontal action

was fixed at 0.4 times the vertical one, as exceeding this value could have reduced the resistant section of the joint due to the load's eccentricity.

Each test yielded data in tabular form, as in table 2, containing the readings from the two extensometers and three displacement transducers, as well as the load applied by the jack. The relative force-displacement diagrams were thereby plotted for the direction parallel to the isolation joint, together with the corresponding hysteresis cycles undergone by each single sample.

RESULTS

Mechanical behavior.

The trials revealed an overall mechanical behavior evolving through three distinct stages, more or less apparent depending upon the magnitude of the vertical load and the strength of the mortar:

Stage 1 (elastic): the isolating joint manifests an essentially elastic response, with nearly complete continuity between the foundation and base of the masonry element, so that the integrity of the cut-wall was guaranteed;

Stage 2 (elastomer slip): the elastomer sheath shows early signs of slipping between the two connection edges, though signs of damage either to the block or the mortar joint are lacking; a corresponding fall in the shear stiffness of the isolation layer is observed;

Stage 3 (mortar rupture): the isolation joint is affected by growing cracks; the fractures occur along the vertical direction or somewhat inclined to it, depending upon the axial loads applied. In the latter case (inclined cracks), a generalized increase in the joint's transverse stiffness is observed. This is due to the formation of compressed zones within the joint itself which favor a post-elastic "reticular" response on the part of the mortar-vertical reinforcement assembly.

The role of the vertical reinforcement rods, tested for a maximum a/g ratio of 0.4, results to be decisive for the proper functioning of the isolating device because, in contrast to previous similar proposals, they insure a nearly complete return of the slip plane to its initial configuration. For its part, the elastomer sheath imparts an appreciable degree of transverse slipping to the joint in the absence of hardening. The joint mortar, on the other hand, provides considerable energy dissipation subsequent to the formation of cracks, while at the same time benefiting from the effective post-elastic strengthening effect afforded by the compressed zones, thereby granting considerable load-bearing capacity to the joint even under high-stress conditions.

Rheological model

A rheological model has been developed in order to aid in the interpretation of the data obtained (fig. 6). Briefly, the model represents the joint as a series of elastic-plastic restraints, whose characteristics vary through the three stages observed during the tests. On the basis of the experimental results, each of the structural elements was assigned a proper stiffness K and limit values of the slip coefficient C . In the cases where stiffness was recovered due to the formation of compressed zones, a supplemental elastic restraint, K_p , active in the presence of assigned transverse displacements, was added. Overall, the apparent stiffness relative to the start of each test is given by

$$K_{sp1} = K_{b,eq} + 1 / (1 / K_m + 1 / K_g)$$

in which $K_{b,eq}$ is the portion of the stiffness consequent to the sample's reinforcing rods, K_m is that due to the mortar joint, while K_g is the stiffness contributed by the waterproofing sheath. Moreover, at limit state and when compressed zones are present, the rheological model calls for an increase in stiffness defined by

$$K_{sp3} = K_{b,eq} + K_p$$

in which K_p is the experimental stiffness of the mortar compressed zone.

The annexed table present as sample the calculations of the stiffness contributed by both the sheathing-mortar combination ($K_c=1/[1/K_m + 1/K_g]$), as well as the mortar one (K_p) and the steel rods. It can be seen that the transverse stiffness afforded by this last element is supplemented by a circular ring of mortar that maintains its connection to the rod throughout the test.

The thickness of this ring, assessed under the constraining assumption of a perfect fit sliding at the two ends of the cast, ranges between 6.5 and 8.2 mm.

Seismic analysis of a masonry building.

Lastly, by way of example, a simulation was performed of the effects of such an isolator applied to the base of the simple square-plan masonry building, 12 m on a side, illustrated in annexed figure. The analysis was performed in conformity with the guidelines in Euro Code n.8, using the simplified response spectrum (report 4.1, part 1-1) with type C soil. The center wall, whose total mass is 126,38 tons, is subjected to the greatest stress.

Here, varying degrees of plane shear were obtained depending upon the isolator type used. The values, in fact, varied as a function of the fundamental period of the mass-isolator assembly itself. It was furthermore found that varying the isolator's reinforcement exclusively affected the specific period exhibited by the building. On the other hand, the in-service value of plane shear, above which slipping between the wall and foundation begins to occur, depends essentially on the type of mortar used in the joint. The analyses conducted yielded limit acceleration values of between 0.069 and 0.076 g for the type 1 mortar and from 0.084 to 0.096 g for type 2. These therefore represent the ranges to adopt as the design values when the aim is to maintain the limit in-service state for low-intensity earthquakes, while the hysteresis response should be applied only in the event of seismic events of considerable intensity.

CONCLUSIONS

The proposed base isolating system for masonry buildings examined in the tests described in the foregoing provides a good combination of implementation ease and mechanical properties. It moreover offers the added benefit of waterproofing the building's groundwork, thanks to the insertion of the elastomer sheath. In particular, from the perspective of mechanics, a good deal of design freedom results from its adoption, as the parameters of isolator stiffness and limit strength can be adjusted through quite a wide range, depending on the choice of reinforcement and mortar. In addition, slipping, and the consequent energy dissipation, can be allowed for in the limited cases of earthquakes of certain preset intensities.

The results obtained also show the way for further development and research: more accurate analytical assessments are in fact possible through the development of a suitable mechanical model for the joint, while the possibilities of prefabricating the isolating system by adopting an on-site assembly procedure for its constituent elements appears quite promising. Finally, from the experimental point of view, it would seem opportune to broaden the range of horizontal stresses with respect to the vertical ones, extending the analysis to ratios greater than the rather limited maximum adopted in the present work.

REFERENCES

- Arnold, C. & Reitherman, B. 1989. Bearing masonry and earthquakes – the Imperial Hotel of Tokyo, *Costruire in Laterizio* n.8. Milano: P.E.G..
- Arya, A.S. 1984. Sliding concept for mitigation of earthquake disaster to masonry buildings, *Proc. 8th World Conf. Earthquake Eng.*, San Francisco.
- Buckle, G. & Mayes, R. 1990. Seismic Isolation: History, Application and Performance – A world view, *Earthquake Spectra*, Vol.6, n.2.
- Kelly, J.M..1986. Aseismic base isolation: review and bibliography. *Soil Dynamics and Earthquake Engineering*, Vol.5, n.4.
- Li, L. 1984. Base isolation measure for aseismic buildings in China, *Proc. 8th World Conf. Earthquake Eng.*, San Francisco.
- Olariu, L. 1994. Passive control and base isolation: state of the art lecture, *Proc. 10th European Conf. Earthquake Eng.*, Wien.
- Sassu, M. 1999. A non conventional device for energy dissipation on masonry buildings: the reinforced cut-wall, *Proc. Int. Workshop ASSISI-99*, Assisi. CICOP: Firenze.
- Zhou, F.L. 1993. Most recent developments on seismic isolation of civil buildings and bridges in P.R.China, *Proc. Int. Post-S.M.I.R.T. Conf. Seminar*, Capri.
- Zhou, F.L., Lu, X., Wang, Q., Feng D. & Yao, Q. 1998. Dynamic analysis on structures base isolated by a ball

system with restoring property, *Earthquake Engineering and Structural Dynamics*, n.27.

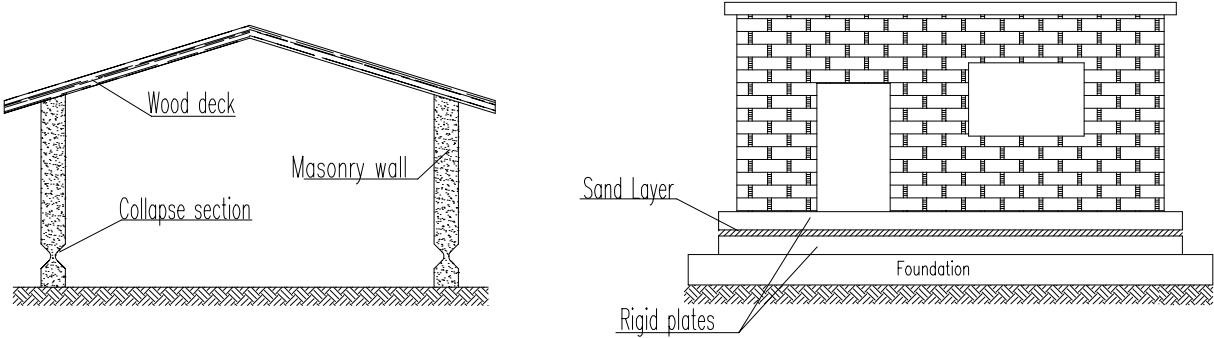
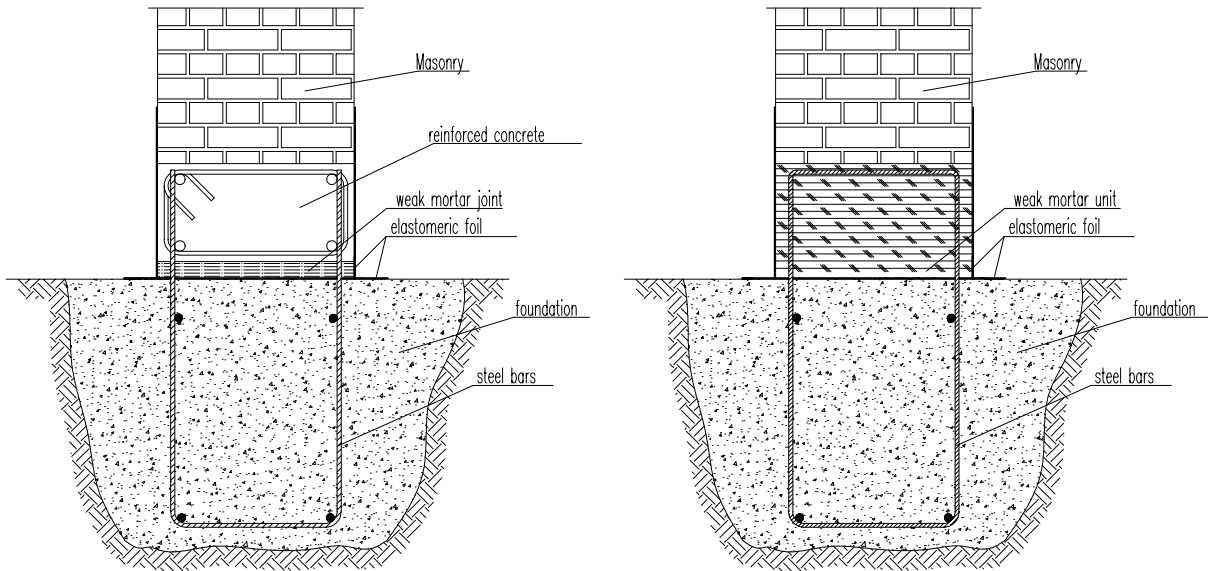


fig.1: Examples of distributed base-isolation



**fig.2: Schemes of reinforced cut-wall:
(a)-small displacement, (b)- large displacements.**

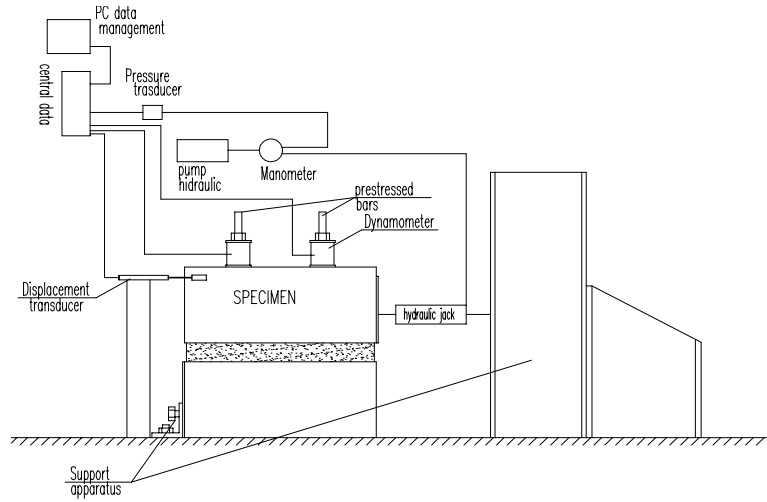


fig.3: Scheme of apparatus trials.

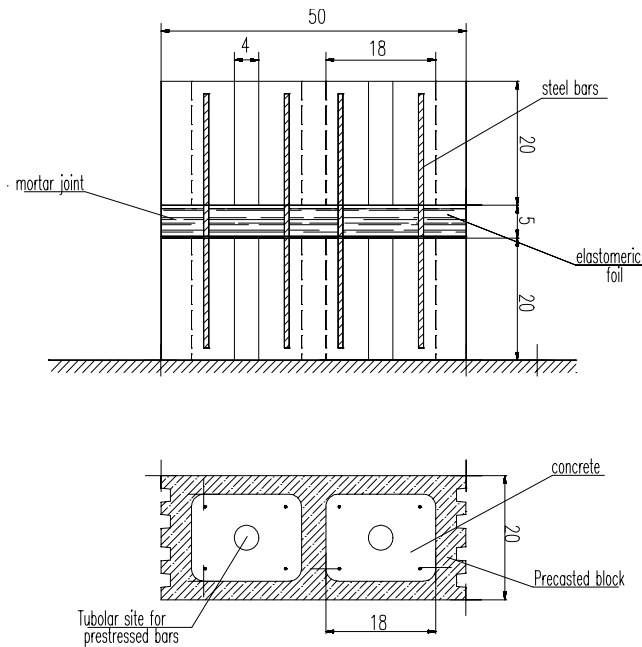


fig.4: Specimen geometry

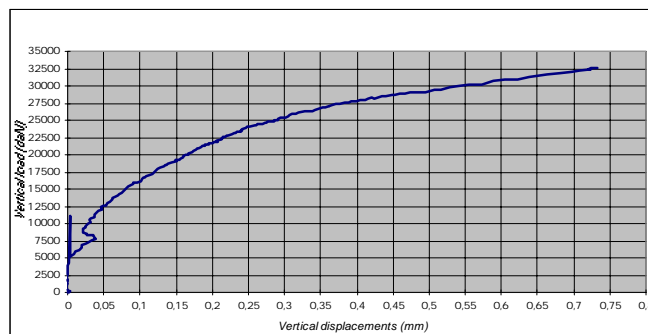


fig.5: Compression test of base isolator

Trial data: specimen 6	
Mortar type:	1
Vertical load:	5 kg/cmq
Width jack:	27,5 cm

reading n.	red Extens. 1/1000mm	white Extens. 1/1000mm	central Extens. 1/1000mm	Horizontal load daN	Dynamometer 02 daN	Dynamometer 00 daN	Average horizontal displacement mm	Total vertical load daN	Notes
1	32	-91	-20	0	-2505	-2480	0,0	-4985	1° cycle
2	466	96	236	520	-2441	-2478	0,29	-4919	
3	974	385	596	1050	-2415	-2530	0,68	-4945	
4	1561	756	1047	1500	-2376	-2593	1,15	-4969	
5	1472	749	1044	1050	-2363	-2568	1,11	-4931	
6	1004	494	739	570	-2363	-2466	0,77	-4829	
7	281	57	214	0	-2376	-2376	0,21	-4752	
8	737	294	502	515	-2363	-2441	0,54	-4804	2° cycle
9	1211	571	834	1015	-2363	-2504	0,90	-4867	
10	1590	781	1082	1500	-2350	-2568	1,18	-4918	
11	1486	762	1064	1020	-2337	-2543	1,13	-4880	
12	1026	511	759	550	-2350	-2466	0,79	-4816	
13	299	67	229	0	-2363	-2376	0,22	-4739	
14	769	318	534	530	-2350	-2428	0,57	-4778	3° cycle
15	1244	596	864	1000	-2337	-2504	0,93	-4841	
16	1617	806	1108	1500	-2337	-2568	1,20	-4905	
17	1526	796	1097	1050	-2337	-2543	1,17	-4880	
18	1029	512	764	550	-2324	-2453	0,79	-4778	
19	330	83	247	0	-2350	-2364	0,25	-4714	
20	773	319	539	515	-2337	-2414	0,57	-4751	4° cycle
21	1264	613	885	1020	-2337	-2491	0,95	-4828	
22	1635	818	1126	1500	-2324	-2568	1,22	-4892	
23	1533	801	1102	1050	-2324	-2543	1,17	-4867	
24	1023	507	757	540	-2324	-2453	0,79	-4778	
25	298	64	226	0	-2350	-2364	0,22	-4714	
26	825	355	583	530	-2324	-2428	0,61	-4753	5° cycle
27	1318	655	931	1030	-2324	-2504	0,99	-4828	
28	1667	845	1163	1500	-2310	-2580	1,25	-4891	
29	1524	803	1113	1030	-2310	-2530	1,17	-4840	
30	1048	524	777	570	-2324	-2441	0,81	-4765	
31	360	103	273	0	-2337	-2351	0,27	-4688	
32	793	343	566	510	-2324	-2402	0,59	-4726	6° cycle
33	1300	650	926	1030	-2310	-2491	0,99	-4801	
34	1677	862	1173	1500	-2310	-2568	1,26	-4878	
35	1474	783	1072	960	-2310	-2517	1,14	-4828	
36	685	306	516	300	-2310	-2389	0,53	-4699	
37	303	66	232	0	-2324	-2339	0,23	-4663	

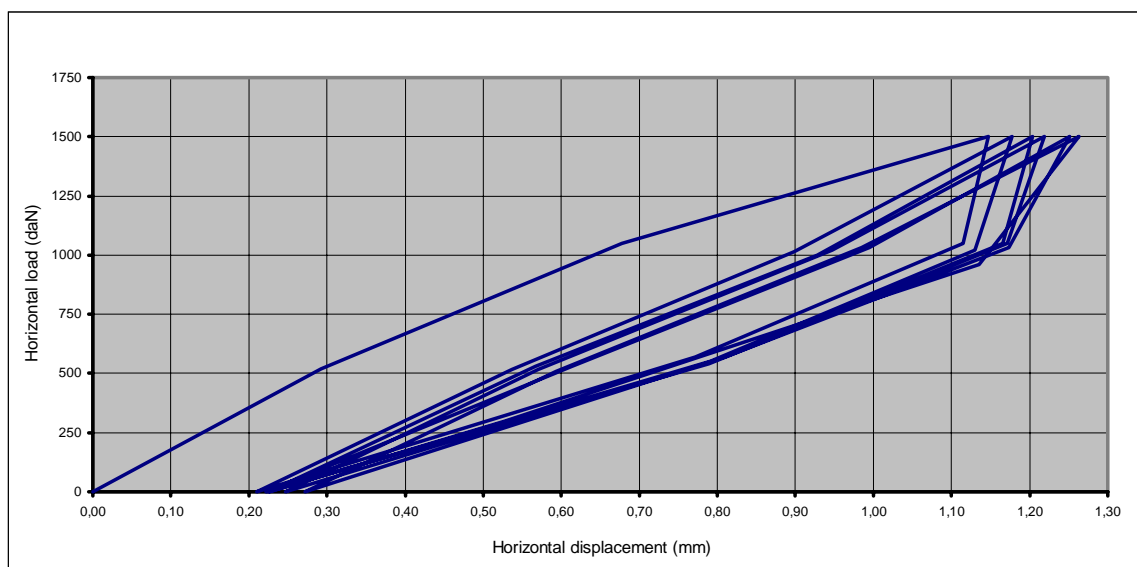


table 2: Technical schedule on specimen n. 6/mortar type 1

Specimen n° 4: 4φ8						Specimen n° 6: 4φ12					
n. cycle	Experimental stiffness phase 1 K_{sp1}	Experimental stiffness phase 2 $K_{sp2}=K_b.eq$	stiffness steel bars phase 3 K_e	stiffness phase 4 $K_{sp3}=K_b.eq+K_p$	Incremental phase 4 stiffness K_p	n. cycle	Experimental stiffness phase 1 K_{sp1}	Experimental stiffness phase 2 $K_{sp2}=K_b.eq$	stiffness steel bars phase 3 K_e	stiffness phase 4 $K_{sp3}=K_b.eq+K_p$	Incremental phases 4 stiffness K_p
1	9298	5698	3600	2784	-2914	1	17931	13590	4341	9574	-4016
2	8306	8015	291	9231	1216	2	15606	13889	1717	17321	3432
3	7606	7569	37	10435	2866	3	15588	13056	2532	17857	4801
4	7746	7059	687	12368	5309	4	16094	13289	2805	17778	4489
5	7123	7083	40	12051	4968	5	13590	13158	432	18077	4919
6	8281	6761	1520	11395	4634	6	15938	13333	2605	16786	3453

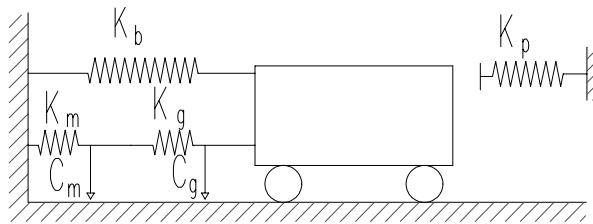
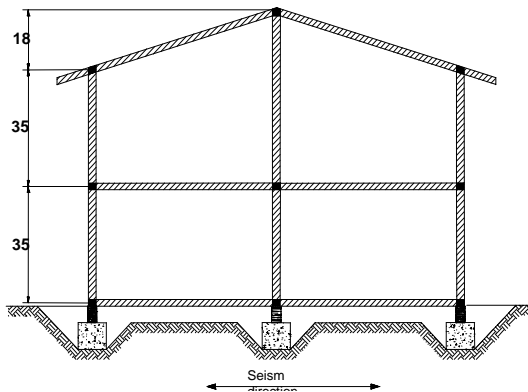


fig.6: Rheological model of base isolator.



isolator type	mortar type	stiffness phase 1 (daN/cm)	fundamental period (sec.)	Total shear force (daN)	Shear force of single b.i.	a/g phase 1	Shear force of single b.i. phase 1
1	2	43525	0,0697	28037	1168,2	0,086	502
2	2	33801	0,0791	28750	1197,9	0,084	503
3	2	57153	0,0609	27364	1140,2	0,088	502
4	2	92958	0,0477	26367	1098,6	0,091	500
5	2	210879	0,0317	25151	1048,0	0,096	503
6	2	170325	0,0353	25422	1059,3	0,088	466

Fig.7: Applicative example (EC8- static method)